Structure of Nonevaporating Sprays, Part I: Initial Conditions and Mean Properties

A.S.P. Solomon,* J-S. Shuen,† Q-F. Zhang,‡ and G. M. Faeth§
The Pennsylvania State University, University Park, Pennsylvania

Structure measurements were completed within the dilute portion of axisymmetric nonevaporating sprays. Measurements included: mean velocities, velocity fluctuations, and Reynolds stress of the gas phase; and mean velocities, fluctuating velocities, mass flux, and diameter distributions of the drop phase. The measurements were used to evaluate three typical methods of analyzing sprays: 1) a locally homogeneous flow (LHF) analysis, where slip between the phases is neglected; 2) a deterministic separated flow (DSF) analysis, where slip is considered but effects of drop interactions with turbulence are ignored; and 3) a stochastic separated flow (SSF) analysis, where effects of both slip and turbulence are considered using random-walk computations for drop motion. Measurements of initial conditions of both phases near the injector, mean gas-phase properties, and liquid flux distributions are described herein. Best agreement between predictions and measurements was obtained with the SSF model, which provided a reasonable representation of turbulent dispersion of drops. A companion paper presents additional measurements of drop continuous phase properties.

Nomenclature

d = injector diameter
d_p = drop diameter
G = liquid mass flux
k = turbulence kinetic energy
r = radial distance
u = axial velocity
v = radial velocity
x = axial distance
ϵ = rate of dissipation of turbulence kinetic energy
ρ = density
ϕ = generic property

Subscripts

c = centerline quantity
p = drop property
0 = injector exit condition

Superscripts

$( )''$ = Favre-averaged fluctuating quantity
$(\tilde{})$ = Favre-averaged quantity
$(\bar{})',(\bar{})$ = time-averaged quantity

Introduction

THE objective of this investigation was to complete measurements of the structure of the dilute portion of axisymmetric nonevaporating sprays injected into a still air environment, in order to provide information on the properties of this flow as well as data useful for the evaluation of spray models. This configuration has a simple geometry, boundary conditions are well defined, and initial conditions needed for calculations were measured; therefore, the measurements should be useful for model evaluation. The new data were also used to begin model evaluation, considering several methods typical of recent spray analyses.

Early studies of the structure of nonevaporating sprays are described in recent reviews by Faeth[1] and Crowe.[2] Since that time, new measurements have been reported by several investigators.[3-7] Alpert and Mathews[3] present some measurements for nonevaporating spray configurations encountered in sprinkler systems and point out the need for additional measurements in sprays. Popper et al.[4] measured mean velocities of both phases in a round turbulent two-phase jet, but drop sizes were not accurately determined, and the loading of the dispersed phase was low in comparison to practical sprays. Yule et al.[5] report measurements in nonevaporating sprays in a coflowing stream; however, unusually well-atomized sprays were considered (mass mean drop sizes of 10-30 μm in the major portion of the spray), and measurements of drop size were only roughly correlated with drop velocities. Tishkoff and co-workers[6,7] treated nonevaporating sprays in a coflowing stream—measuring drop sizes and velocities at several positions in the sprays; however, continuous-phase velocities were not measured. Bracco and co-workers[8,9] recently report drop-velocity measurements in nonevaporating sprays injected into pressurized nitrogen atmospheres, along with analysis of these results. However, drop sizes and properties of the continuous phase were not measured directly.

The present investigation supplements these studies, considering properties of both phases for sprays having significant interaction between the phases. The structure measurements included: mean and fluctuating gas velocities and Reynolds stress, using laser Doppler anemometry (LDA); combined drop sizes and velocities, using multiflash photography; drop sizes using slide impaction and Fraunhofer diffraction; and liquid mass fluxes using isokinetic sampling.

The new data were employed to evaluate three representative spray models: 1) a locally homogeneous flow (LHF) model, where velocity differences (slip) between the phases were neglected; 2) a deterministic separated flow (DSF)

Received May 14, 1984; revision received Dec. 7, 1984.

*Research Assistant, Department of Mechanical Engineering; currently Senior Research Engineer, General Motors Research Laboratories, Warren, MI.

†Research Assistant, Department of Mechanical Engineering; currently Senior Research Engineer, Sverdrup Technology Inc., Cleveland, OH.

‡Adjunct Lecturer, Department of Mechanical Engineering; currently Lecturer, Department of Aero-Engine, Nanjing Aeronautical Institute, Nanjing, China.

§Professor, Department of Mechanical Engineering; currently Professor, Department of Aerospace Engineering, University of Michigan, Ann Arbor, MI. Associate Fellow AIAA.

model, where slip was considered but effects of drop interactions with turbulence and turbulent dispersion of drops were ignored; and 3) a stochastic separated flow (SSF) model, where effects of interphase slip, turbulent fluctuations, and turbulent dispersion were considered, using random sampling for turbulence properties in conjunction with random-walk computations for drop motion. These models were developed in this laboratory and evaluated earlier, using data obtained for monodisperse particle-laden jets.[10-13] The present investigation extends the evaluation to sprays where effects of polydisperse size distributions, smaller length scales, higher levels of particle loading, and greater rates of flow deceleration, typical of practical sprays, are encountered.

The paper begins with a discussion of the test arrangement and experimental methods. This is followed by a brief description of the LHF, DSF, and SSF models. More complete details concerning these models are available elsewhere.[11] The paper concludes with a discussion of spray structure near the injector and comparison of predicted and measured mean properties of both phases. A companion paper presents additional measurements of drop properties as well as the turbulence properties of the gas phase.[14] Full details of all aspects of the study and a complete tabulation of data are provided by Solomon.[15]

Experimental Methods

Test Apparatus

The apparatus (Fig. 1) consisted of an air-atomizing injector (see Table 1 for specifications) injecting vertically downward within a screened enclosure (one layer of 16-mesh screen 1 m square and 2.5 m high) to reduce effects of room disturbances. Since optical instrumentation was mounted rigidly, the injector was traversed to obtain profiles of flow quantities—two directions using the injector mount and the third major traverse by moving the screened enclosure. The inlet of the exhaust system was screened and located 1 m below the plane of the measurements. Tests showed that operation of the exhaust system had negligible (less than 1%) influence on flow properties at the measuring plane.

The injector delivered a full-cone spray with no swirl and is identical to the ones used by Shearer et al.[10] Airflow to the injector was metered and controlled with a critical flow orifice and pressure regulator. The spray liquid was vacuum pump oil in order to eliminate effects of evaporation due to its low volatility (see Table 1 for specifications). The liquid was fed to the injector by pressurizing the fuel tank with air. The tank was not agitated and pressure levels were moderate (0.3-0.8 MPa); therefore, the dissolved air content of the liquid was negligible. The liquid flow was metered with a rotameter. In order to maintain repeatable atomization conditions, the test area was heated to above-normal temperature (300 ± 1 K) so that liquid properties remained constant over the time of testing.

Table 1 Summary of test conditions[a]

	Air jet	Sprays Case 1	Sprays Case 2
Injected fluids	Air	Air and oil[b]	Air and oil[b]
Injector flow rates, mg/s			
Gas	338	338	216
Liquid	0	600	1400
Loading ratio[c]	0	1.78	6.48
Jet momentum, mN	120.1	137.2	70.1
Initial velocity, m/s[d]	175	146	43.4
Reynolds number[d], $\times 10^4$	2.6	3.0	2.4
SMD, μm[e]	—	30	87
Spray angle[f]	—	30	33

[a] All flows employ Spraying Systems air-atomizing injector (Model 1/4J2050 nozzle, No. 67147 air nozzle, 1.194-mm injector exit diameter). Ambient and injector inlet temperature, 300 ± 1 K; ambient pressure, 97 kPa.

[b] Sargent-Welch Scientific Co., Duo Seal Oil Catalog No. 1407K25, density = 878 kg/m^3, vapor pressure at 38°C = 4×10^{-4} mm Hg.

[c] Ratio of injected liquid to gas flow rates.

[d] Assuming LHF: The viscosity of air was employed for the Reynolds number.

[e] Measured with the Malvern Model 2200 particle sizer at $x/d = 12.6$ with 9-mm laser beam diameter.

[f] Determined from liquid flux measurements at $x/d = 50$.

Test Conditions

Three test conditions were used: 1) a pure air jet, formed by the injector, to serve as a baseline; 2) a spray having a nominal Sauter mean diameter (SMD) of 30 μm, similar to the spray studied by Shearer et al.[10]; and 3) a spray having a SMD of 87 μm, which exhibited significant effects of slip. The specifications of the three test conditions are summarized in Table 1.

Injector operation was monitored continuously by measuring drop sizes with a Malvern model 2200-particle sizer. This instrument operates on the principle of Fraunhofer diffraction of laser light. The measuring region of the instrument included the entire spray width, centered at $x/d = 12.6$, with the input laser beam having a diameter of 9 mm. Injector properties were also monitored by periodically measuring injector thrust with an impact plate placed at $x/d = 21$, as in past work.[10] Spray angles were found from liquid flux measurements (taken as the angle form the injector exit which bounds the region where the liquid mass flux is greater than 1% of its centerline value at $x/d = 50$).

Instrumentation

Gas Velocity

Mean and fluctuating gas velocities were measured with a dual-beam, single-channel, frequency-shifted LDA, using several beam orientations to provide measurements of various velocity components and the Reynolds stress. The optical configuration yielded a measuring volume having length and diameter of 470 and 98 μm with a fringe spacing of 3.13 μm.

LDA seeding particles were provided in two ways: 1) the surroundings were seeded using oil droplets generated from the exhaust of a vacuum pump (0.6-μm average diameter with a concentration of 3×10^{10} particles/m^3); and 2) the smallest drops in the spray after eliminating erroneous signals from large drops by setting a low signal-amplitude limit on the counter data processor. In the region where LDA measurements were made ($x/d > 40$), photographic measurements showed that the maximum concentration of spray drops was roughly 3×10^9 drops/m^3 for the most finely atomized spray tested. In general, the concentration of spray drops was two orders of magnitude less than the concentration of seeding particles—minimizing effects of bias due to spray drops. Concentration bias was eliminated by adjusting external seeding until intermittency was no longer observed on the oscillograph trace of the LDA detector output. Signal rates were high; therefore, the low-pass-filtered analog output of the burst counter was time-averaged using an integrating digital voltmeter (in conjunction with a true rms voltmeter for fluctuating velocities). It is estimated that mean and fluctuating velocities have an uncertainty less than 10%. All LDA measurements were repeatable within 5% over the several-months period of testing.

Liquid Flux

Liquid flux was measured with an isokinetic sampling probe operating at the mean gas velocity (measured using the LDA). The probe had a 3-mm i.d. sampling port followed by a gas-flushed diverging section to prevent premature drop impact on probe surfaces. The drops were captured on a composite filter (No. 2 Whatman filter paper separated by

layers of gauze and cotton), which was weighed before and after collection of liquid (scale sensitivity of 1 mg). Sampling times were in the range 1-10 min—depending on location in the spray. Integration of liquid mass flux measurements over spray cross sections agreed with injected liquid flow rates within 15% and uncertainties in this measurement are the same.

Drop Size and Velocity Correlation

A double-flash shadow photographic method, similar to that of McCreath et al.,[16] was used for combined measurements of drop size and velocity. The arrangement consists of two submicrosecond flash sources (General Radio Type 1538 Strobotac and Type 1539-A Stroboslave, having flash durations of 500 and 800 ns, respectively), a lens system to focus the light, and a camera—all on the same optical axis. The flashes were fired consecutively (firing intervals of 2-80 μs) so that two images of the drops were obtained on the same photograph, with one image darker than the other, in order to resolve drop size, velocity, and direction (negative velocities of small drops are encountered near the edge of the sprays due to flow reversals).

Various configurations of camera lenses, film, and data reduction methods were used in different regions of the sprays. For $x/d=50$, a Graphlex 4×5 still camera (3000 ASA Polaroid Type 57 film, 38:1 primary magnification, 2.3×2.3 mm field of view) was used with images analyzed under a calibrated microscope. For $x/d\geq100$, a 35-mm camera back (50-1600 ASA, Agfa Pan Vario-XL Professional 35-mm film, 6:1 primary magnification ratio, 5.7×8.0 mm field of view) was used with images analyzed after projection on a screen at greatly increased magnification. The depth of field in which droplets appear to be in focus in the optical sampling volume increases with increasing drop size. The depth of field was determined as a function of camera optics and drop size so that the drop-size distribution could be corrected for depth-of-field bias.[15]

The accuracy of drop-velocity measurements was estimated to be within 10%. Uncertainties in drop-size measurements were: 10% for $d_p>25$ μm and 25% for d_p in the range 10-25 μm. The smallest sizes measured were 10 μm diameter. To find drop size and velocity and velocity fluctuation distributions at each location, 600-800 drops were measured. Since the number frequency of large drops ($d_p>50$ and 100 μm for the case 1 and case 2 sprays, respectively) at a given location was relatively low, measurements of fluctuating velocities for these sizes are only qualitative. SMD data obtained by imaging and slide impaction agreed within 15%, suggesting only moderate effects of velocity bias for present test conditions.

Drop Size

In addition to Fraunhofer diffraction (used to monitor the sprays) and flash photography (used for drop-size and velocity correlations), the slide impaction technique was also employed for drop-size measurements. Slide impaction involves momentarily exposing small glass slides coated with a layer of magnesium oxide to the flow using a pneumatically driven shutter.[10] Impacting drops leave a crater in the coating which can be related to initial drop size.[17] The measured sample was corrected for the collection efficiency of the probe following Ranz.[18] Typically, 2000 drops were counted at each measurement location to find the local drop-size distribution and SMD. This is sufficient to determine SMD with an uncertainty less than 10%, limited primarily by the drop sizing determination.

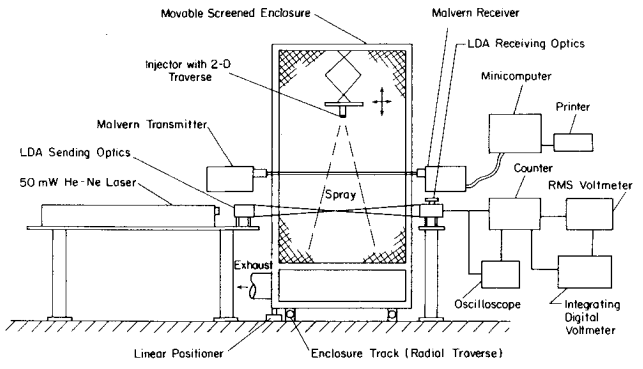

Fig. 1 Sketch of the experimental apparatus.

Theoretical Methods

General Description

Theoretical methods will only be briefly discussed, since a full description has been reported in connection with work on monodisperse particle-laden jets.[13] The major difference between the present study and Ref. 13 involves the need to sum over several (typically 10) drop-size groups for polydisperse sprays.

The test conditions correspond to steady axisymmetric boundary-layer flows. Mach numbers are low; therefore, kinetic energy and viscous dissipation of the mean flow, as well as gas density variations, were neglected with little error. Both the density and the mass flow rate, at any axial station, of the liquid phase are constant. Other assumptions vary for the LHF, DSF, and SSF models and will be treated separately below.

To find the properties of the continuous phase, a k-ϵ-g and a k-ϵ model were used for the LHF and separated flow analyses, respectively. This approach yielded good predictions of mean and turbulence properties in constant- and variable-density single-phase jets during past work.[1,10-15,19,20]

LHF Model

The LHF approximation implies that both phases have the same local velocity; therefore, the flow corresponds to a variable-density single-phase fluid due to changes in liquid concentration, even though the density of each phase remains constant. The analysis employed Favre-averaged governing equations rather than the time-averaged equations used in earlier work.[10] This allowed use of a single set of empirical constants for both constant- and variable-density flows.[13] The calculations employ the conserved scalar approach described by Lockwood and Naguib,[19] using a clipped-Gaussian function for the Favre probability density function of mixture fraction.

The LHF model does not require detailed information concerning drop sizes and velocities at the initial condition of the flow—which is one of the main advantages of this approach. Therefore, LHF calculations were begun at the injector exit with initial conditions specified following past practice.[10-15] Methods of computation were also the same as past work in this laboratory.[10-15]

Structure predictions and measurements are presented as Favre-averaged properties, defined as follows:

$$\tilde{\phi}=\overline{\rho\phi}/\bar{\rho} \tag{1}$$

This procedure is necessary in order to represent predictions of the LHF model correctly. This distinction is of no consequence, however, concerning measurements of phase properties and predictions of the separated flow models, since the density of each phase is constant and Favre and time averages are formally identical.

DSF Model

Both separated flow models adopt the main features of the LHF model, but only for the gas phase. The liquid phase was treated by solving Lagrangian equations of motion for

the drops and then computing source terms due to interphase transport which appear in the governing equations for the gas phase. This involves dividing the drops into groups, defined by diameter, velocity, and position at the initial condition, and then computing their subsequent motion through the flowfield.

Initial conditions for the separated flow models were specified at $x/d = 50$, which was the position nearest the injector where all needed measurements could be made with acceptable spatial resolution and accuracy. Downstream of this position, the void fraction was always greater than 99.1%; therefore, the volume of the liquid phase and drop collisions could be ignored with little error. The exchange of momentum between the phases was considered as a source term in the governing equation for conservation of momentum for the gas phase.

Direct effects of drop motion on turbulence properties (called turbulence modulation by Al Taweel and Landau[21]) were ignored in the results presented in this paper since the comparison between measurements and predictions was limited to the dilute spray region. Experimental observations of turbulence modulation effects in and near the dense spray regions, as well as preliminary analysis using the SSF model to estimate the effect of turbulence modulation, are presented in the companion paper.[14]

The main assumptions of the drop trajectory calculations were as follows: since the flow was dilute, effects of adjacent drops on drop drag were ignored; drag was treated empirically, assuming spherical drops in a quasisteady flow; since $\rho_p/\rho \approx 750$, effects of virtual mass, Basset forces, Magnus forces, etc., were neglected with little error; ambient conditions for drops were taken to be local mean flow properties, and effects of velocity fluctuations on drop drag were ignored; and turbulent dispersion of drops was also ignored. These assumptions are typical of deterministic separated flow models of dilute sprays and are discussed more completely elsewhere.[1]

SSF Model

Like the DSF model, the SSF model involves solving Lagrangian equations of motion for drops and the computing source terms due to interphase transport which appear in the governing equations for the gas phase.

The stochastic separated flow model treats effects of turbulent fluctuations on interphase momentum transport rates and turbulent dispersion of drops using a technique proposed by Gosman and Ioannides[22] and subsequently developed in this laboratory.[11-13] This involves computing trajectories of a statistically significant sample of individual drops (typically 4000-6000) as they move away from the injector and encounter a succession of turbulent eddies—utilizing Monte Carlo methods.

Properties within a particular eddy are assumed to be uniform but to change in a random fashion from eddy to eddy. Trajectory calculations are the same as the DSF model, except that instantaneous eddy properties replace mean-gas properties.

Eddy properties are found by making a random selection from the probability density function (pdf) of velocity—assuming isotropic turbulence. A drop is assumed to interact with an eddy as long as its relative displacement is less than a characteristic eddy size and its time of interaction is less than the characteristic eddy lifetime. All of these parameters are found directly from the k-ϵ computations with minimal additional empiricism.[11-13]

Results and Discussion

Air Jet

Present measurements of mean and fluctuating velocities were in good agreement with earlier measurements by Shearer et al.[10] using the same twin-fluid injector. The comparison between predictions and measurements was also satisfactory, establishing a single-phase baseline for subsequent work with sprays.[15]

Sprays

Initial Conditions

Flash photographs indicated that irregular sheets and ligaments of liquid were present along with drops in the near-injector region. Since this does not comply with the

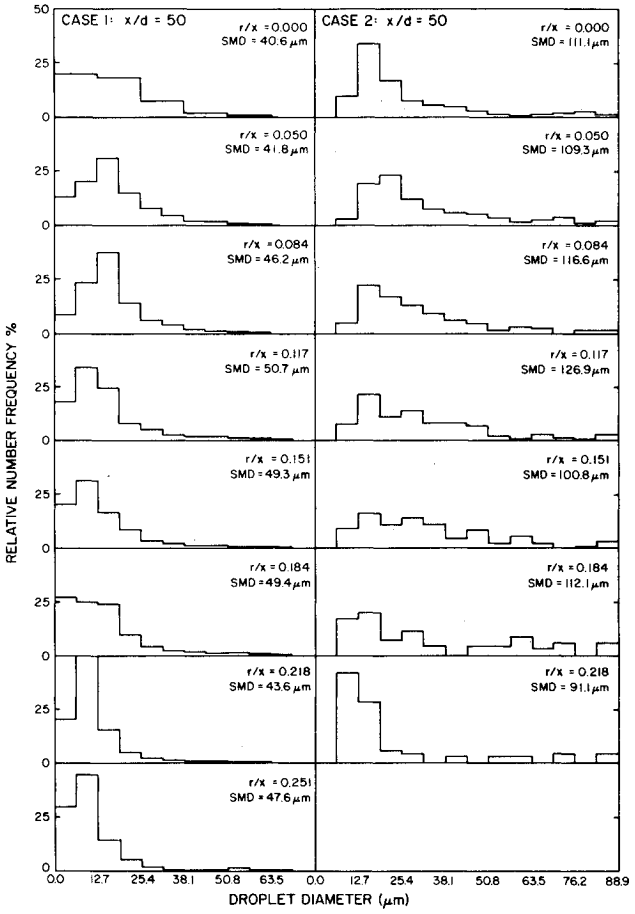

Fig. 2 Drop-size distributions at $x/d = 50$ by slide impaction.

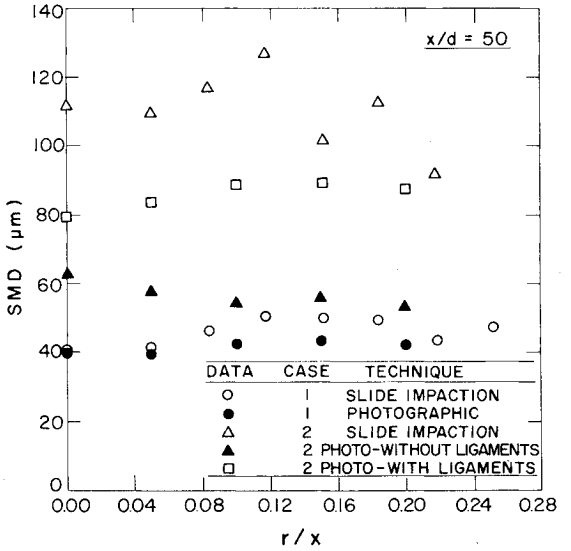

Fig. 3 Radial variation of SMD at $x/d = 50$.

flow configuration (drops) used in the separated flow analyses, initial conditions for the DSF and SSF calculations were measured at $x/d=50$, where effects of ligaments were relatively small and spatial resolution was adequate. These measurements included: drop-size distributions, mean and fluctuating axial drop velocities, liquid flux, and mean and fluctuating velocities and Reynolds stress of the gas phase. These measurements are sufficient to establish initial profiles of k and ϵ—the latter by inversion of the turbulence model; i.e., the initial Reynolds stress distribution is matched.

Figure 2 is an illustration of slide impaction measurements of drop-size distributions for various radial positions at $x/d=50$. The flash photography results are similar.[15] The observed drop-size ranges extend to 120 and 200 μm for the case 1 and case 2 sprays, respectively; but the number frequencies in these size ranges are too small to be shown on Fig. 2. The radial distributions of SMD computed from both slide impaction and flash photography measurements are illustrated in Fig. 3. Although the size distributions differ in detail at various radial positions, the SMD was relatively uniform across both sprays. The SMD values measured at $x/d=50$ are greater than the normal size obtained by the Fraunhofer diffraction measurements at $x/d=12.6$. This could be due to the presence of ligaments near the injector, which undoubtedly biases the Fraunhofer diffraction method, as well as the increase in drop sizes by collisions and coalescence in the dense portion of the sprays—postulated by O'Rourke and Bracco.[23]

The SMD values obtained by slide impaction and flash photography, illustrated in Fig. 3, are nearly the same for the case 1 spray. Since the present slide impaction measurements are closer to a time average while flash photography is a spatial average, this agreement should only formally hold when the velocities of all drops are the same. Drop-velocity measurements at $x/d=50$ for this spray, illustrated in Fig. 4, indicate that this is not the case (the larger drops have higher velocities at this position, which should result in a larger SMD from the slide impaction measurements). However, SMD is strongly dominated by the largest drops in the distribution, whose velocities do not vary greatly with size for this spray; therefore, the SMD is nearly the same for the two methods. Separated flow calculations require time-averaged drop properties; therefore, the slide impaction measurements were used to specify the drop-size distribution at $x/d=50$ for the case 1 spray.

In contrast, flash photographs showed the presence of some ligaments in the case 2 spray at $x/d=50$, corresponding to 20-25% of the mass flux of liquid at each radial location. Ignoring the presence of ligaments, shown in Fig. 3, significantly reduced the measured SMD of the spray. Ligaments were not observed at $x/d=100$; therefore, for the purposes of separated flow computations, the ligaments were broken down into a distribution of drops at $x/d=50$, with the help of the jet breakup theories presented by Reitz[24] and a knowledge of maximum stable drop diameter from measurements downstream of $x/d=50$.[15] The corrected size distribution agreed reasonably well with the slide impactor measurements (see Fig. 3), although irregular ligament breakup at the inlet of the impact probe undoubtedly influenced the latter measurements to some degree. Therefore, the corrected photographic measurements were used to specify initial drop-size distributions for the case 2 spray instead of the slide impactor measurements. Naturally, the presence of ligaments at the initial condition introduces greater uncertainties in model evaluation for the case 2 spray.

The SMD measurements, illustrated in Fig. 3, show that drops were observed in these sprays for $r/x>0.2$, which is beyond the edge of most fully developed single-phase jets.[1,10] This effect is attributable to initial radial velocities produced by the injector, dispersion of drops by turbulent fluctuations, and drop shattering and collisions in the dense portion of the spray. The effect of turbulent dispersion of drops, which is a dilute-spray mechanism, will be considered later.

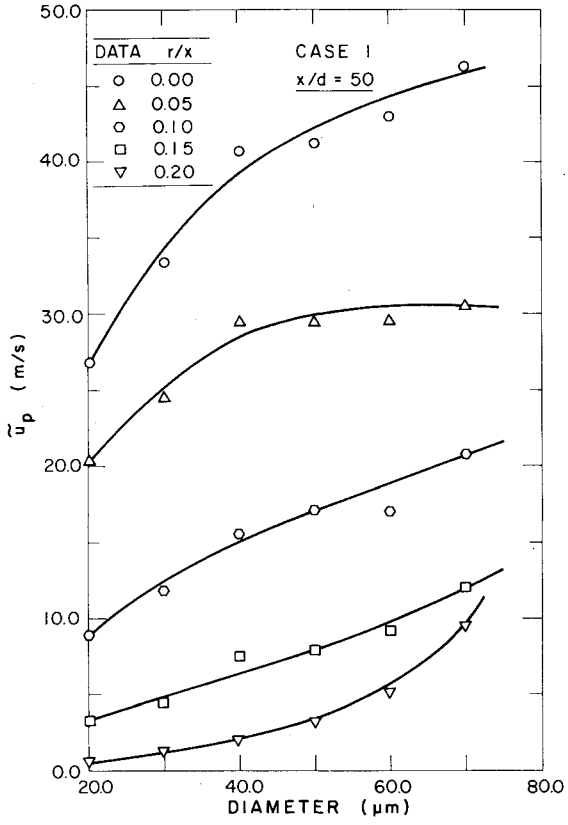

Fig. 4 Correlation of mean streamwise drop velocity and size for the case 1 spray at $x/d=50$.

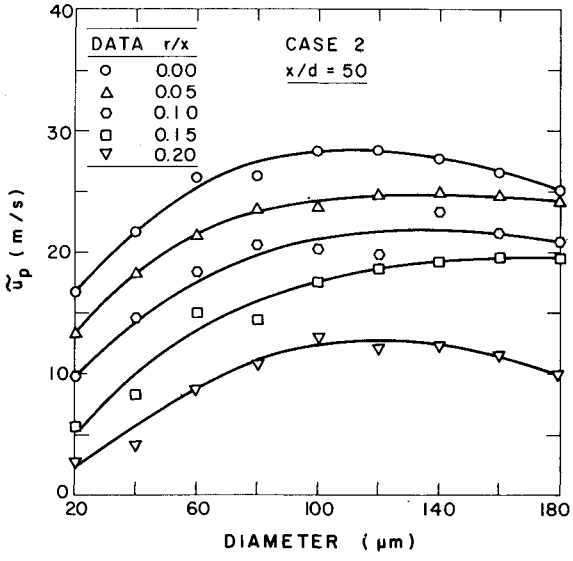

Fig. 5 Correlation of mean streamwise drop velocity and size for the case 2 spray at $x/d=50$.

Mean drop velocities at $x/d=50$, as a function of drop size and radial position, are illustrated in Figs. 4 and 5. For the case 1 spray (Fig. 4), mean axial velocity increases with drop size, as noted earlier. In contrast, drop velocities for diameters greater than 100 μm are relatively uniform for the case 2 spray. This size range is dominated by drops formed by the late breakup of ligaments; therefore, these drops tend to maintain ligament velocities since they have had little time to respond to the drag of the flow.

In general, small drops ($d_p < 30$ μm) had mean velocities 10-90% *lower* than mean gas velocities. This behavior may be due to the turbulent dispersion of small drops from the edge of the flow toward the axis. Recirculation of small drops near the edge of the flow was also observed at times. The large drops ($d_p > 30$ μm), however, had mean velocities 10-300% larger than the local gas velocity at any given radial position. The mean velocity data illustrated in Figs. 4 and 5 were used directly to specify initial drop properties for separated flow calculations.

Streamwise drop-velocity fluctuations at $x/d = 50$ for the case 1 spray are illustrated in Fig. 6. Values vary irregularly; however, streamwise drop-velocity fluctuations generally increase with drop size as they do with mean velocities (see Fig. 4). Fluctuations relative to the centerline mean drop velocity were in the range 25-40% at the axis, decreasing to 2-10% at the edge of the spray. Streamwise drop velocity fluctuations for the case 2 spray were less systematic, probably due to late breakup of ligaments, with values in the range 3-7 m/s.[15] The measured correlations were used to fix initial conditions for separated flow calculations.

The resolution of the photographic technique did not provide measurements of mean and fluctuating radial velocities. Hence, for separated flow calculations, the initial mean radial velocity was assumed to increase linearly from the spray axis to the edge of the flow, matching the spray angle at the latter condition, viz., $\tilde{v}_p = 0.7\tilde{u}_p r/x$. Initial fluctuating radial velocities were specified to be a fixed ratio of the fluctuating axial velocities, viz., $(\tilde{v}_p''^2)^{1/2} = (\tilde{u}_p''^2)^{1/2}/3$. These prescriptions agree with limited observations that could be made and also provided the best match for SSF model predictions downstream of $x/d = 50$.

Conditions of Predictions

The following results are presented as Favre averages in order to conform to the output of the LHF model. As noted earlier, Favre and time averages are equivalent for the properties of each phase since the density of each phase is constant. Few results are presented for the DSF model, since this approach was not very successful for the present sprays.

Uncertainties in initial conditions at $x/d = 50$ influence predictions of the separated flow models. Specific results of sensitivity analysis are discussed in Ref. 14 after all measurements have been described. In general, uncertainties in the separated flow calculations due to uncertainties in initial conditions are comparable to the uncertainties of the measurements.

Centerline Properties

Predicted (LHF and SSF models) and measured mean gas velocities along the axis of the two sprays are illustrated in Fig. 7. Mean gas velocities decay at a somewhat slower rate than single-phase jets due to exchange of momentum from the drop phase. Increased drop loading for the case 2 spray results in a downstream shift of the velocity-decay curve. This effect is analogous to an extension of the potential-core region of a single-phase jet when the density of the injected flow is greater than the ambient density.[1] The LHF model predictions follow these trends but overestimate the rate of decay of velocity, similar to the findings of Shearer et al.[10] Errors in LHF predictions increase as the SMD of the spray increases, indicating that the difficulty is due to ignoring effects of slip. This conclusion is supported by the fact that the SSF model, which allows for slip, provides satisfactory predictions of mean centerline velocities for both sprays.

Similar results for mean liquid mass flux are illustrated in Fig. 8. This is one of the most sensitive spray properties, decreasing almost quadratically with increasing distance from the injector. The LHF predictions do not approach the measurements until large values of x/d are reached, where effects of interphase slip are reduced. The SSF model, however, provides reasonably good predictions in the range of x/d where it was used. SSF predictions and measurements are in poorest agreement at the measuring location farthest from the injector; however, experimental accuracy was also poorest at this position, which may be a factor in the comparison.[15]

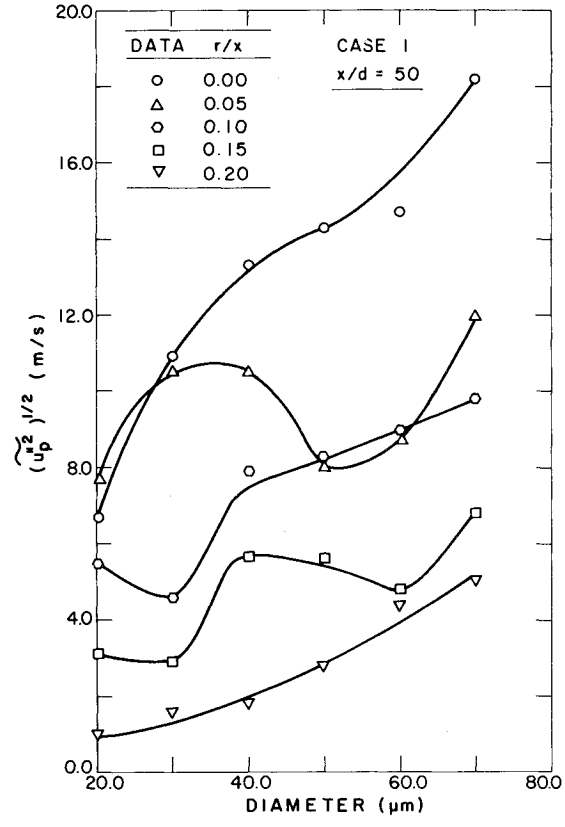

Fig. 6 Correlation of streamwise drop-velocity fluctuations and size for the case 1 spray at $x/d = 50$.

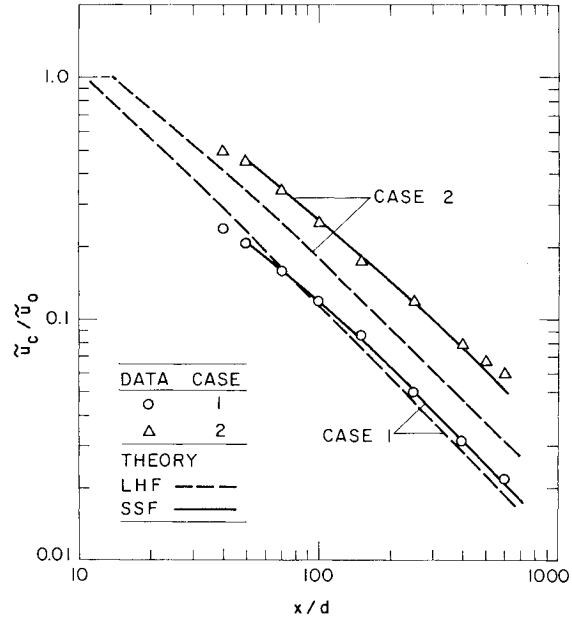

Fig. 7 Mean gas-phase velocities along the spray axis.

Radial Profiles

Predicted (LHF and SSF models) and measured radial profiles of mean streamwise gas velocities, including the in-

itial condition at $x/d=50$, are illustrated in Fig. 9. Radial distances are normalized by the distance from the injector, which is the similarity variable for single-phase jets,[1] in order to illustrate predictions of flow width directly. These results illustrate an interesting property of the test sprays (and probably other sprays as well). During computations for particle-laden jets,[11-13] the LHF model invariably overestimated the width of the flow since neglecting slip causes the rate of dispersion of large particles by turbulent fluctuations to be overestimated. In the present case, however, the sprays spread more rapidly than the LHF prediction due to enhanced turbulent dispersion of drops. The increased dispersion of drops in the present sprays, in comparison to the earlier particle-laden jet results,[11-13] can be attributed to: 1) the smaller density of the drops; 2) the greater rates of flow deceleration due to the smaller injector dimensions of the sprays; and 3) the larger initial slip between the phases in sprays. The effect of enhanced spreading is greatest near the injector, in spite of the fact that this is a region where characteristic relaxation times of turbulent fluctuations are small in comparison to characteristic relaxation times of drop motion; therefore, this process is an important property of the dense-spray region. Far from the injector, response times of the drops become small in comparison to the gas phase, which tends to improve the LHF approximation so that this approach performs better. It is very encouraging that the SSF model reproduces this unexpected effect reasonably well, with no change in modeling procedure or empirical constants.

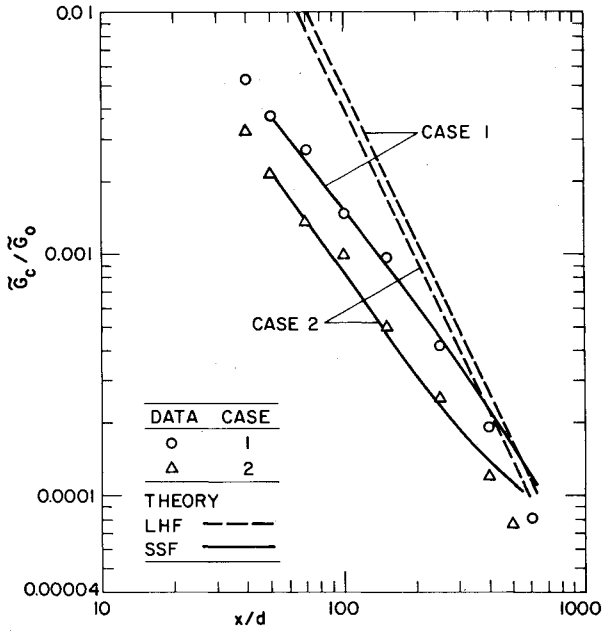

Fig. 8 Mean liquid flux along the spray axis.

Predicted and measured radial profiles of liquid mass flux are illustrated in Fig. 10. In this case, predictions from all three methods of analysis are shown. The DSF model yields poor results, similar to particle-laden jets.[11-13] Neglecting drop dispersion by turbulence causes the rate of spread of the flow to be substantially underestimated, even after allowing for the apparent radial velocity of the drops at $x/d=50$. Another undesirable feature of the DSF model is that radial deflection of drops can only result from mean radial gas velocities, as with laminar two-phase flows.[25] As a result, the DSF model predicts that drops accumulate at an off-axis position where $\tilde{v}=0$ and radial motion is stable, e.g., $\tilde{v}>0$ for positions nearer the axis while $\tilde{v}<0$ for larger radial distances, which for turbulent jets is typically at $r/x=0.06$-0.10.[26] Since $(\tilde{v}''^2)^{1/2} \gg \tilde{v}$ in most turbulent jet flows, this behavior is not observed in the present sprays because effects of turbulent dispersion dominate the radial spread rates of drops.

The LHF model is not subject to the turbulent dispersion deficiency of the DSF model and provides better prediction

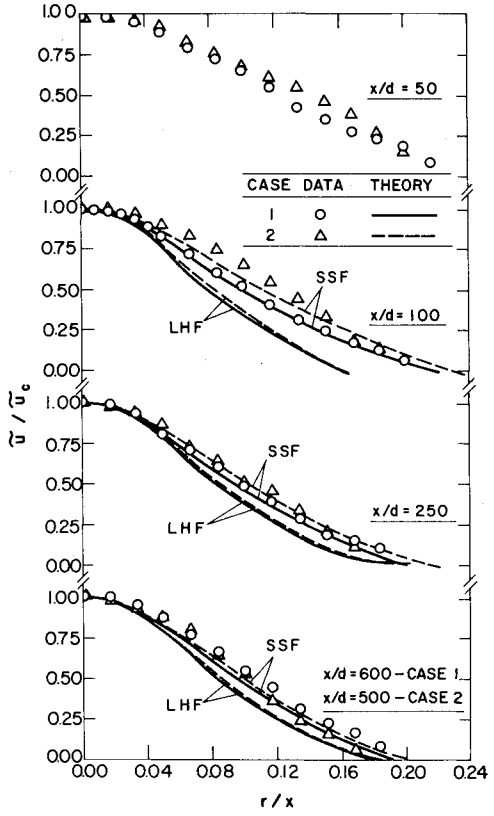

Fig. 9 Radial variation of mean gas-phase velocity.

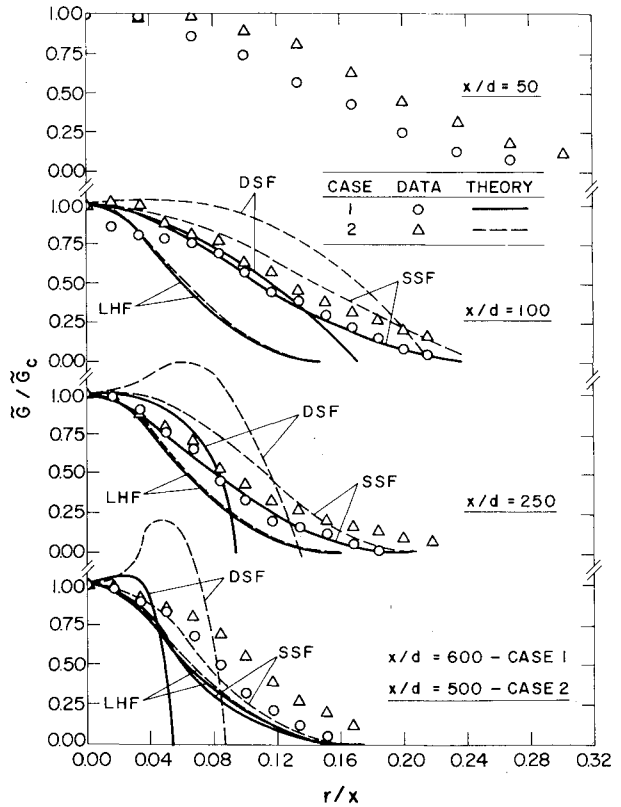

Fig. 10 Radial variation of mean liquid flux.

of the liquid mass flux profiles in Fig. 10—particularly far from the injector, where effects of slip become small. On the other hand, the SSF model, which allows for both slip and turbulent dispersion, provides the best predictions of liquid mass flux profiles. The performance of the SSF model, however, is poorer for liquid flux than for other measurements considered during this study. Subsequent sensitivity study shows that liquid flux predictions are particularly sensitive to estimates of initial conditions[14]; therefore, this may be a potential source for these errors.

Summary and Conclusions

New experiments of the structure of the dilute portions of nonevaporating sprays in a still environment were completed. Three typical spray models were both evaluated and used to help interpret the measurements, as follows: 1) a locally homogeneous flow (LHF) model, where slip between the phases is neglected; 2) a deterministic separated flow (DSF) model, where slip is considered but effects of turbulent fluctuations and particle dispersion are ignored; and 3) a stochastic separated flow (SSF) model, where effects of both slip and turbulent dispersion are considered. The present paper describes near-injector properties, which are used to specify initial conditions for separated flow calculations, as well as mean gas velocities and liquid flux throughout the flow. A companion paper considers mean and fluctuating drop velocities, drop-size distributions, and gas-phase turbulence properties in the dilute-spray region.[14]

Final conclusions will be withheld pending discussion of the remaining measurements in Ref. 14, however, several observations can be made based on the results presented here, as follows:

1) The present measurements in nonevaporating sprays showed significant effects of slip and turbulent dispersion of drops—the latter effect yielding spray widths that were larger than fully developed single-phase jets. In the dense spray regions, drop shattering and collisions probably also contribute to rapid spread rates.

2) The LHF model generally overestimates the rate of flow development of the sprays, as in past experience.[1,10-13] However, the LHF model *underestimated* flow widths—unlike results in particle-laden jets—due to enhanced turbulent dispersion; therefore, the LHF model does not always provide an upper bound on flow widths—as suggested in the past.[1]

3) The DSF model generally underestimated flow widths and drop spread even though it required the full input of a separated flow model. This approach appears to have limited utility for analysis of practical sprays, although Gosman and Ioannides[22] note that uncertainties in initial conditions for multiphase flows often cause greater errors than neglecting particle/turbulence interactions.

4) The SSF model yielded encouraging structure predictions for the present sprays, including effects of enhanced turbulent dispersion, with no changes from the version developed using results for particle-laden jets.[11-13]

5) Both the Fraunhofer diffraction method and the slide impactor gave no obvious indication that ligaments were present at the initial condition location of the case 2 spray; therefore, these techniques should be supplemented by direct imaging in order to provide a more reliable indication of the nature of sprays.

Acknowledgments

This research was sponsored by the National Aeronautics and Space Administration, Grant NAG 3-190, under the technical management of R. Tacina of the Lewis Research Center.

References

[1]Faeth, G. M., "Evaporation and Combustion of Sprays," *Progress in Energy and Combustion Science*, Vol. 9, Jan. 1983, pp. 1-76.

[2]Crowe, C. T., "Review—Numerical Methods for Dilute Gas-Particle Flows," *Journal of Fluids Engineering*, Vol. 104, 1982, pp. 197-303.

[3]Alpert, R. L., and Mathews, M. K. "Calculation of Large-Scale Flow Fields Induced by Droplet Sprays," *Polyphase Flow and Transport Technology*, ASME, NY, 1980, pp. 112-128.

[4]Popper, K., Abuaf, N., and Hetsroni, G., "Velocity Measurements in a Two-Phase Turbulent Jet," *International Journal of Multiphase Flow*, Vol. 1, Jan. 1974, pp. 715-726.

[5]Yule, A. J., Ah Seng, C., Felton, P. G., Ungut, A., and Chigier, N. A., "A Study of Vaporizing Fuel Sprays by Laser Techniques," *Combustion and Flame*, Vol. 44, Jan. 1982, pp. 71-84.

[6]Tishkoff, J. M., Hammond, D. C. Jr., and Chraplyvy, A. R., "Diagnostic Measurements of Fuel Spray Dispersion," *Journal of Fluids Engineering*, Vol. 104, Sept. 1982, pp. 313-317.

[7]Tishkoff, J. M., "Measurements of Particle Size and Velocity in a Fuel Spray," *Second International Conference on Liquid Atomization and Spray Systems*, Madison, WI, June 1982.

[8]Martinelli, L., Reitz, R. D., and Bracco, F. V., "Comparisons of Computed and Measured Dense Spray Jets," *Proceedings of Ninth International Colloquium on Dynamics of Explosions and Reactive Systems*, Poitiers, France, July 1983.

[9]Wu, K-J., Santavicca, D. A., Bracco, F. V., and Coghe, A., "LDV Measurements of Drop Velocity in Diesel-Type Sprays," *AIAA Journal*, Vol. 22, Sept. 1984, pp. 1263-1270.

[10]Shearer, A. J., Tamura, H., and Faeth, G. M., "Evaluation of a Locally Homogeneous Flow Model of Spray Evaporation," *Journal of Energy*, Vol. 3, Sept.-Oct. 1979, pp. 271-278.

[11]Shuen, J-S., Chen, L-D., and Faeth, G. M., "Evaluation of a Stochastic Model of Particle Dispersion in a Turbulent Round Jet," *AIChE Journal*, Vol. 29, Jan. 1983, pp. 167-170.

[12]Shuen, J-S., Chen, L-D., and Faeth, G. M., "Predictions of the Structure of Turbulent, Particle-Laden Jets," *AIAA Journal*, Vol. 21, Nov. 1983, pp. 1483-1484.

[13]Shuen, J-S., Solomon, A.S.P., Zhang, Q-F., and Faeth, G. M., "Structure of Particle-Laden Jets: Measurements and Predictions," *AIAA Journal*, Vol. 23, March 1985, pp. 396-404.

[14]Solomon, A.S.P., Shuen, J-S., Zhang, Q-F., and Faeth, G. M., "Structure of Nonevaporating Sprays, Part II: Drop and Turbulence Properties," *AIAA Journal*, in press.

[15]Solomon, A.S.P., "A Theoretical and Experimental Study of Turbulent Sprays," Ph.D. Thesis, The Pennsylvania State University, University Park, PA, 1984.

[16]McCreath, C. G., Roett, M. F., and Chigier, N. A., "A Technique for Measurement of Velocities and Size Particles in Flames," *Journal of Physics E: Scientific Instruments*, Vol. 5, 1972, pp. 601-604.

[17]May, K. R., "The Measurement of Airborne Droplets by the Magnesium Oxide Method," *Journal of Scientific Instrumentation*, Vol. 27, 1950, pp. 128-130.

[18]Ranz, W. F., "Principles of Inertial Impaction," The Pennsylvania State University, University Park, PA, Research Bulletin 13-66, 1956.

[19]Lockwood, F. C. and Naguib, A. S., "The Prediction of the Fluctuations in the Properties of Free, Round Jet, Turbulent, Diffusion Flames," *Combustion and Flame*, Vol. 24, Feb. 1975, pp. 109-124.

[20]Gosman, A. D., Lockwood, F. C., and Syed, S. A., "Prediction of a Horizontal Free Turbulent Diffusion Flame," *Proceedings of the Sixteenth Symposium (International) on Combustion*, The Combustion Institute, Pittsburgh, PA, 1977, pp. 1543-1555.

[21]Al Taweel, A. M. and Landau, J., "Turbulence Modulation in Two-Phase Jets," *International Journal of Multiphase Flow*, Vol. 3, June 1977, pp. 341-351.

[22]Gosman, A. D. and Ioannides, E., "Aspects of Computer Simulation of Liquid-Fueled Combustors," AIAA Paper 81-0323, 1981.

[23]O'Rourke, P. J. and Bracco, F. V., "Modelling of Drop Interactions in Thick Sprays and a Comparison with Experiments," *Proceedings of the Institute of Mechanical Engineers Conference on Stratified Charge Engines*, Nov. 1980, pp. 101-116.

[24]Reitz, R. D., "Atomization and Other Breakup Regimes in a Liquid Jet," Ph.D. Thesis 1375-T, Princeton University, Princeton, NJ, 1978.

[25]Soo, S. L., *Fluid Dynamics of Multiphase Systems*, Blaisdell, Waltham, MA, 1967.

[26]Abramovich, G. N., *The Theory of Turbulent Jets*, M.I.T. Press, Cambridge, MA, 1963, p. 82.